Hyperfine Interact (2016) 237:41
DOI 10.1007/s10751-016-1241-5

Spin canting in ferrite nanoparticles

J. Marx[1] · H. Huang[1] · K. S. M. Salih[1] · W. R. Thiel[1] · V. Schünemann[1]

Abstract Recently, an easily scalable process for the production of small (3−7 nm) monodisperse superparamagnetic ferrite nanoparticles $MeFe_2O_4$ (Me = Zn, Mn, Co) from iron metal and octanoic acid has been reported (Salih et al., Chem. Mater. **25** 1430–1435 2013). Here we present a Mössbauer spectroscopic study of these ferrite nanoparticles in external magnetic fields of up to B = 5 T at liquid helium temperatures. Our analysis shows that all three systems show a comparable inversion degree and the cationic distribution for the tetrahedral A and the octahedral B sites has been determined to $(Zn_{0.19}Fe_{0.81})^A[Zn_{0.81}Fe_{1.19}]^BO_4$, $(Mn_{0.15}Fe_{0.85})^A[Mn_{0.85}Fe_{1.15}]^BO_4$ and $(Co_{0.27}Fe_{0.73})^A[Co_{0.73}Fe_{1.27}]^BO_4$. Spin canting occurs presumably in the B-sites and spin canting angles of 33°, 51° and 59° have been determined for the zinc, the manganese, and the cobalt ferrite nanoparticles.

Keywords Spin canting · Iron oxide nanoparticles · Ferrite · Mössbauer spectroscopy · Catalysis

1 Introduction

One of the main reasons for the emergence of nanotechnology in recent time is that physical properties of small structures differ from the properties of their bulk material [1]. This is in many cases due to surface effects dominating in very small structures with sizes in the range of a few nanometers. One of these surface effects is spin-canting, an effect that leads

This article is part of the Topical Collection on *Proceedings of the International Conference on the Applications of the Mössbauer Effect (ICAME 2015), Hamburg, Germany, 13–18 September 2015*

✉ J. Marx
jmarx@physik.uni-kl.de

[1] Department of Physics, University of Kaiserslautern, Erwin-Schrödinger-Str. 46, 67663 Kaiserslautern, Germany

Published online: 22 February 2016

to a different net magnetization in small particles because of a different orientation of the surface ions' spins [2]. Spin canting has been observed in a variety of spinels and it is still not absolutely clear whether spin canting in ultrasmall nanometer-sized particles occurs only at the surface but also in the inner core of these particles. A possibility to measure the amount of canted spins is Mössbauer spectroscopy with a large applied external field, in which the bulk ions' spins, but not the surface ions' spins align. In the following paper we present a study on zinc, manganese and cobalt ferrite nanoparticles which have been prepared by means of a new preparation route directly from metal powders and octanoic acid by thermolysis in a high-boiling solvent [3].

2 Materials and methods

Highly crystalline manganese-, zinc- and cobalt-ferrite nanoparticles were synthesized as described in [3]. Mössbauer spectroscopy was performed in a setup as described in [4] with a closed-cycle helium cryostat (Cryo Industries of America, Inc.) equipped with a superconducting magnet with a maximal field of 5 T, oriented parallel to the γ-radiation. Spectra were taken in constant acceleration mode, and analyzed using least mean square fits. Isomer shifts are quoted relative to α-Fe Mössbauer spectra were analyzed with the Vinda Macro [5], using Lorentzian doublets and sextets.

3 Results and discussion

The room-temperature Mössbauer spectra of the three ferrite samples are shown in Fig. 1. The Mössbauer parameters of the $ZnFe_2O_4$ NPs (Fig. 1a; $\delta = 0.37$ mm/s, QS $= 0.60$ mm/s) are comparable to those observed for 11 nm nanostructured zinc ferrite prepared by high energy ball milling [6] and to 10 nm zinc ferrite NPs synthesized from ferric nitrate solution [7]. It can be concluded that the small particle sizes (3-7 nm, [3]) lead to a fast superparamagnetic relaxation resulting in doublets at room temperature. We attribute the observed deviations from lorentzian line shape to those particles, which do not relax faster than the Mössbauer time window of $\sim 10^{-7}$ s. For $MnFe_2O_4$ NPs a quadrupole splitting of 0.57 mm/s is observed (Fig. 1b), which is slightly lower than the value 0.72 mm/s reported for the core of 2 nm manganese ferrite on porous MCM-41 silica support [8]. Also the quadrupole splitting of the $CoFe_2O_4$ NPs (QS=0.53 mm/s) is slightly lower than that reported of 5 nm cobalt ferrite NPs prepared by coprecipitation (0.76 mm/s).

Lower temperatures lead to a slower relaxation and a splitting to sextets [9], which can be seen in Fig. 3. All samples have two components in the low-temperature, low-field spectra, resulting from the different sites in the ferrite sublattice, as shown in Fig. 2. High-field Mössbauer spectra, taken at 5 K with an applied parallel field of 5 T for the $ZnFe_2O_4$, $MnFe_2O_4$ and $CoFe_2O_4$ are shown in Fig. 3a-c. Each of the high-field spectra has been analyzed by three components. It is assumed that two of these components result from the two different sublattice positions, A-sites and B-sites, in ferrites, as depicted in Fig. 2. These components show a line ratio of 3:0:1:1:0:3. The third component represents the canted spins, the line ratio of this component is 3:p:1:1:p:3, where p is the polarization value that is used to calculate the spin-canting angle [10]. The parameters for the three samples are all listed in Table 1. Sextet A represents the ferric iron oxide in the tetrahedral sublattice, as can be seen from the larger hyperfine-field splitting, which is due to the parallel orientation of the internal hyperfine-field in the external field. Sextet B represents ferric iron oxide

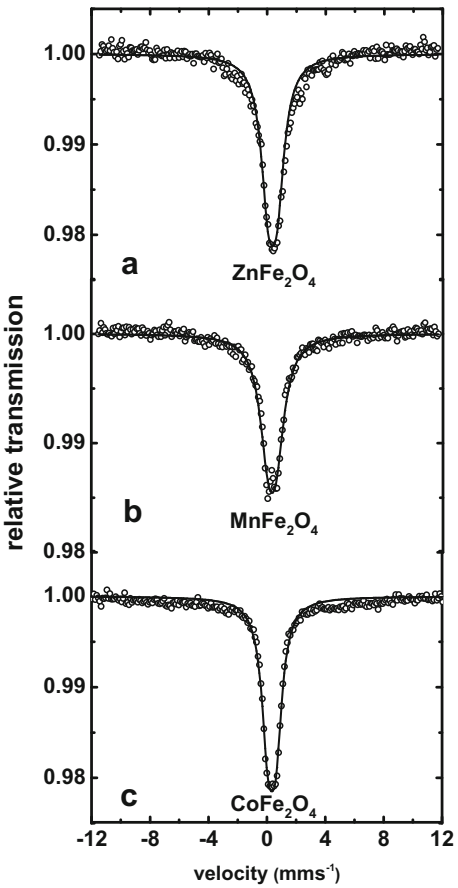

Fig. 1 Zero field Mössbauer Spectra of $ZnFe_2O_4$ (**a**), $MnFe_2O_4$ (**b**) and $CoFe_2O_4$ (**c**) nanoparticles, measured at 300K. The solid lines are fits with $\delta =$ 0.37 mm/s, QS = 0.60 mm/s, and $\Gamma = 1.2$ mm/s for (**a**), $\delta = 0.34$ mm/s, QS = 0.57 mm/s and $\Gamma =$ 1.38 mm/s for (**b**), $\delta = 0.35$ mm/s, QS = 0.53 mm/s, $\Gamma =$ 1.05 mm/s for (**c**)

in the octahedral sublattice, as can be seen from the smaller B_{hf} due to an antiparallel orientation of the internal hyperfine field in the external field [11, 12]. The third sextet, the spin-canting component, has parameters similar those of sextet B, therefore we conclude that this component most likely represents ferric iron oxide in the octahedral sublattice, as it was observed for spin canting in ferrites [10, 13, 14]. This might result from a different coordination of the surface ions due to less iron coordination possibilities [15].

The $ZnFe_2O_4$ particles (Fig. 3a,d) have a spin-canting component with a relative area of 24 %. The calculated spin-canting angle is 33°. An exceptional high occupation of A-sites with Fe(III), with an inversion parameter of i = 0.81, compared to bulk $ZnFe_2O_4$ with a normal spinel occupation (i.e. i = 0), could be seen in the 5 T spectrum, which would also explain the magnetic properties and the high saturation magnetization of the $ZnFe_2O_4$ nanoparticles in ref. [3].

Chinnasamy et al. have analyzed the Mössbauer spectrum of nanostructured zinc ferrite by means of 3 components similar to the approach presented in this study [6]. For 10 nm nanostructured zinc ferrite they report for iron in B-sites in the grain boundaries a canting angle of 45°. They also report spin canting of the A-and B-sites of the bulk material of 37° and 35 °, respectively. Choi et al. on the other hand investigated zinc ferrite NPs with an average size of 8.8 nm and reported a canting angle of 29° of the B-sites but no canting at

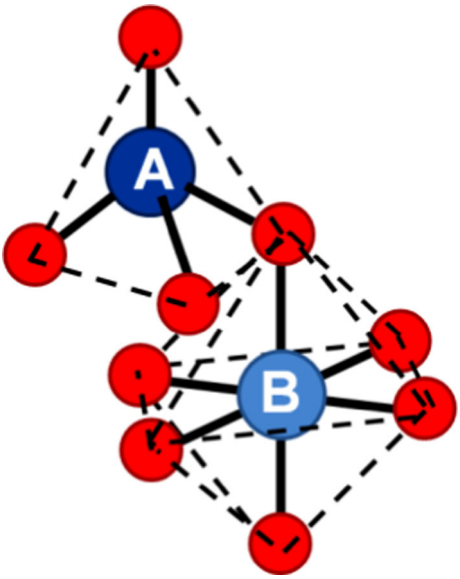

Fig. 2 Schematic sublattice structure of ferrites, with tetrahedral A-sites and octahedral B-sites

the A-sites [16]. Pandey et al have analyzed the field dependent Mössbauer data obtained in field up to 6T by means of one component representing the A-sites and two components for the B-sites [7], they have found a canting angle of 32° for the B2-sites and 57° for the B1-sites.

For the $MnFe_2O_4$ particles, with a slightly smaller sample size distribution of 4-7 nm, the spin-canting component had a relative area of 42 % which is larger than observed for the $ZnFe_2O_4$sample (Fig. 3b,e). The inversion parameter i = 0.85 is in the same range as for the $ZnFe_2O_4$ sample. The determined spin-canting angle is 51° for this sample.

Manganese ferrite particles also prepared by ball milling have also been investigated by Mössbauer spectroscopy in fields of up to 5T [17]. For 82 nm grain sizes a cation distribution $(Mn_{0.55}Fe_{0.45})[Mn_{0.45}Fe_{1.55}]O_4$ with an inversion parameter of i=0.45 has been found. For these particles canting angles for the A sites of 30° and for the B sites of 39° are reported [17].

For the sample with the smallest particle size ($CoFe_2O_4$, 3-5 nm [3], see Fig. 3c,f) the relative area of the spin-canting component is higher than in the two other samples (50 %) whereas the calculated canting angle is 59°. The inversion parameter i = 0.73 is only slightly smaller than found for the other two particle systems.

For 2 nm cobalt ferrite particles prepared by an autocombustion technique Peddis et al. [10] report canting angles of 42° $(Co_{0.80}Fe_{0.20})[Co_{0.20}Fe_{1.80}]O_4$ and 37° $(Co_{0.56}Fe_{0.44})[Co_{0.44}Fe_{1.56}]O_4$. In their study exactly the same fitting model was used as in the present study and the spin canting component was attributed to a surface component with spin canting explicitely seen in octahedral B sites. It should be noted that in a later paper [18] 6 nm cobalt ferrites have been found considerable canting in the range of 40° both for the A and B sites.

For the calculated canting angle, as well as the relative area of the spin-canting component, there is a tendency to a larger relative area for decreasing particle sizes. The increase in the spin-canting component seems to go along with a decrease of the relative area of both sublattice components, site A and site B. As it was shown before that the particles are highly

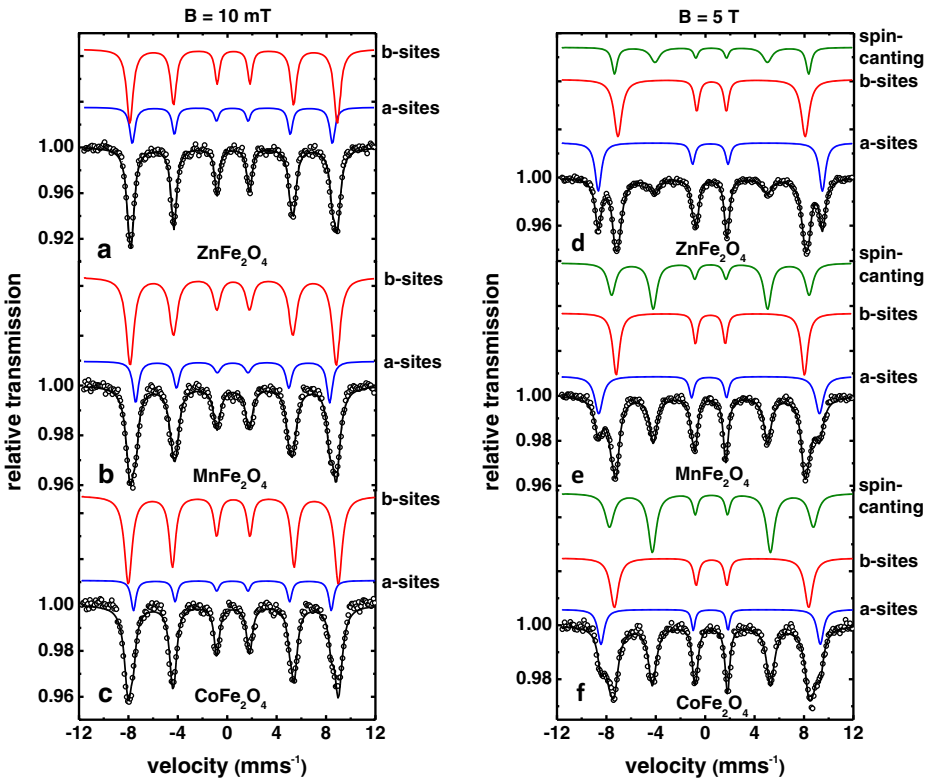

Fig. 3 Low field (10 mT) and high field (5 T) Mössbauer spectra of $ZnFe_2O_4$ (**a/d**), $MnFe_2O_4$ (**b/e**) and $CoFe_2O_4$ (**c/f**) nanoparticles, measured at 5 K. The field direction was parallel to the γ-rays. The solid lines have been obtained by means of a least square fitting analysis assuming lorentzian lineshape and the Mössbauer parameters listed in Table 1

crystalline [3], one may speculate that the larger surface to volume ratio in the smaller particles leads to a larger number of surface ions, and a larger relative area of the spin-canting component in the Mössbauer spectrum.

In the case of pure surface spin canting, a size approximation from the relative surface area would be possible from the obtained areas: If one assumes spherical particles, a pure core-shell-model, a thickness of $e_{cant} = 1$ nm [19] for the canted layer for all 3 samples, the same Lamb-Mössbauer factor for all components, as well as pure surface spin canting, the particle size can be roughly estimated via [20]:

$$\%A = \%V_{shell} = V_{Particle} - V_{core} = 1 - \frac{(d - e_{cant})^3}{d^3} \quad (1)$$

The calculated diameters are plotted against the diameters obtained via transmission electron microscopy (TEM) in Fig. 4. Although the errors are significant (±1-2.5 nm), the size of the $MnFe_2O_4$ and $CoFe_2O_4$ particles are a good approximation of the ones obtained via TEM. However, the size of the $ZnFe_2O_4$ particles is estimated too big by a factor of 2.

In conclusion, a size dependence of the relative area of the spin canting component in the Mössbauer spectra of nm sized cobalt and manganese-ferrite particles, but not of zinc ferrite particles has been indicated. This means that the spin canting at least in the cobalt

Table 1 Parameters obtained from the analysis of the Mössbauer spectra shown in Fig. 3

Sample	Particle size [3]	B_{ext}	Comp.	B_{hf}(T) ± 0.2T	δ (mm/s) ± 0.03 mm/s	2ε (mm/s) ± 0.1 mm/s	Γ (mm/s)	p value (norm.)	Rel. area (%) ± 5 %	cationic distribution $(A_{1-i}B_i)[A_iB_{2-i}]O_4$
$ZnFe_2O_4$	5-7nm	5 T	A	56.1	0.39	0.0	0.6;-;0.5	0	31	$(Zn_{0.19}Fe_{0.81})$
			B	46.8	0.49	0.0	0.8;-;0.5	0	46	$[Zn_{0.81}Fe_{1.19}]$
			canted spin	48.6	0.48	0.0	0.5;0.9;0.4	0.71	24	O_4
		10 mT	A	50.1	0.39	0.0	0.5;0.5;0.5	–	29	–
			B	51.9	0.49	0.0	0.6;0.6;0.5	–	71	
$MnFe_2O_4$	4-7 nm	5 T	A	55.2	0.39	0.0	0.8;-;0.5	0	25	$(Mn_{0.15}Fe_{0.85})$
			B	47.1	0.49	0.0	0.6;-;0.4	0	33	$[Mn_{0.85}Fe_{1.15}]$
			canted spin	49.4	0.50	0.0	0.8;0.7;0.5	1.73	42	O_4
		10 mT	A	48.5	0.42	0.0	0.5;0.6;0.7	–	25	–
			B	51.5	0.46	0.0	0.7;0.8;0.7	–	75	
$CoFe_2O_4$	3-5 nm	5 T	A	55.0	0.44	0.0	0.6;-;0.3	0	18	$(Co_{0.27}Fe_{0.73})$
			B	48.7	0.52	0.0	0.8;-;0.5	0	32	$[Co_{0.73}Fe_{1.27}]$
			canted spin	51.1	0.51	0.0	0.9;0.8;0.5	2.40	50	O_4
		10 mT	A	49.6	0.42	0.0	0.5;0.4;0.4	–	18	–
			B	52.7	0.50	0.0	0.7;0.6; 0.5	–	82	

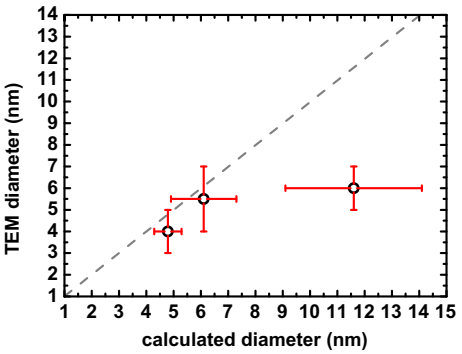

Fig. 4 Particle diameters as obtained by transmission electron microscopy (y-axis), plotted against the diameters obtained from the relative area of the spin canting component (x-axis). Error bars indicate the particle size range as seen in TEM micrographs and as obtained from the surface area in the Mössbauer spectra. The dashed line is solely meant as a guide to the eye

and manganese ferrites investigated here occurres most probably in the B-sites that also preponderate the composition of the particles. It is striking that the inversion degree was shown to be in the same range for all three samples, although the inversion degree of their bulk material differs from a perfect spinel for zinc-ferrite to an almost complete inverted spinel for cobalt-ferrite. This needs certainly further investigation but may be a consequence of the new preparation route since all three ferrite systems have been prepared directly from metal powders by thermolysis.

Acknowledgments This work has been supported by the German Federal Ministry of Education and Research via the research initiative MAGNENZ and by NANOKAT.

References

1. Marx, J., Huang, H., Faus, I., Rackwitz, S., Wolny, J.A., Schlage, K., Wille, H.-C., Schünemann, V.: Hyperfine Interact. **226**, 661–665 (2014)
2. Coey, J.M.D.: Phys. Rev. Lett. **27**(17), 1140–1142 (1971)
3. Salih, K.S.M., Mamone, P., Dörr, G., Bauer, T.O., Brodyanski A., Wagner, C., Kopnarski, M., Klupp Taylor, R.N., Demeshko, S., Meyer, F., Schünemann, V., Ernst, S., Gooßsen, L.J., Thiel, W.R.: Chem. Mater. **25**, 1430.1435 (2013)
4. Janoschka, A., Svenconis, G., Schünemann, V.: J. Phys. Conf. Ser. **217**, 4 (2010)
5. Gunnlaugsson, H.P., Vinda, B.: excel add-on. http://users-phys.au.dk/hpg/vinda.htm. Accessed 10 Sept. 2015
6. Chinnasamy, C.N., Narayanasamy, A., Popandian, N., Chattopadhyay, K., Guérault, H., Greneche, J.-M.: J. Phys.: Condens. Matter **12**, 7795–7805 (2000)
7. Pandey, B., Litterst, F.J., Baggio-Saitovitch, E.M.: J. Mag. Magn. Mater. **385**, 412–417 (2015)
8. Surowiec, Z., Wiertel, M., Gac, W., Budzyński, M.: NUKLEONIKA **60**(1), 137–141 (2015)
9. Bødker, F., Mørup, S., Linderoth, S.: Phys. Rev. Lett. **72**, 282–285 (1994)
10. Peddis, D., Mansilla, M.V., Mørup, S., Cannas, C., Musinu, A., Piccaluga, G., D'Orazio, F., Lucari, F., Fiorani, D.: J. Phys. Chem. B **112**, 8507–8513 (2008)
11. Huang, H., Christmann, R., Ulber, R., Schünemann, V.: Hyperfine Interact. **205**, 121 (2011)
12. Vandenberghe, R.E., De Grave, E.: Mössbauer Effect Studies of Oxidic Spinels. In: Grandjean, F., Long, G.J. (eds.) Mössbauer Spectroscopy Applied to Inorganic Chemistry, vol. 3, p. 59. Plenum Press, New York (1984)
13. Mørup, S., Brok, E., Frandsen, C.: J. Nanomater., 2013, Article ID 720629 8 pages (2013)
14. Baaziz, W., Pichon, B.P., Fleutot, S., Liu, Y., Lefevre, C., Greneche, J.-M., Toumi, M., Mhiri, T., Begin-Colin, S.: J. Phys. Chem. C **118**(7), 3795–3810 (2014)
15. Kodama, R.H., A. E. Berkowitz, A.E., McNiff, E.J.J.r., Foner, S.: Phys. Rev. Lett. **77**(2), 394–397 (1996)

16. Choi, E.J., Ahn, Y., Song, K.-C.: J. Magn. Magn. Mater. **301**, 171–174 (2006)
17. Mahmoud, M.H., Hamdeh, H.H., Ho, J.C., O'Shea, M.J., Walker, J.C.: J. Magn. Magn. Mater. **220**, 139–146 (2000)
18. Peddis, D., Yaacoub, N., Ferretti, M., Martinelli, A., Piccaluga, G., Musinu, A., Cannas, C., Navarra, G., Greneche, J.-M., Fiorani, D.: J. Phys.: Condens. Matter **426004**, 8 pp (2011)
19. Haneda, K., Morrish, A.H.: J. Appl. Phys. **63**, 4258–4260 (1988)
20. Tronc, E., Prené, P., Jolivet, J.P., Dormann, J.L., Grenèche, J.M.: Hyperfine Interact. **112**, 97–100 (1998)